Copyright 2004 by the Society of Photo-Optical Instrumentation Engineers.

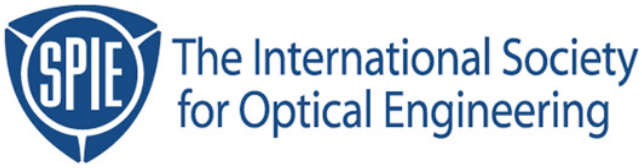

This paper was published in the proceedings of
Optical Microlithography XVII, SPIE Vol. 5377, pp. 428-441.
It is made available as an electronic reprint with permission of SPIE.

One print or electronic copy may be made for personal use only. Systematic or multiple reproduction, distribution to multiple locations via electronic or other means, duplication of any material in this paper for a fee or for commercial purposes, or modification of the content of the paper are prohibited.

Exploring the Capabilities of Immersion Lithography Through Simulation

Chris A. Mack* and Jeffrey D. Byers
KLA-Tencor

ABSTRACT

Immersion lithography has recently emerged as the leading candidate for extending 193nm lithography to the 45nm lithography node and beyond. By immersing the wafer in a high index fluid, lens designs with numerical apertures (NAs) approaching the refractive index of the fluid are possible. While such a high numerical aperture is normally accompanied by an extreme decrease in the depth of focus at the resolution limit, an advantage of the immersion approach to increasing the numerical aperture is that the depth of focus is increased by at least a factor of the refractive index, mitigating some of the DOF loss due to the higher NA and smaller feature. Though this technique for resolution enhancement is receiving significant attention, useful experimental data on the subtle effects of such high NA imaging is one to two years away. Thus, simulation is expected to bridge the gap in immersion lithography research.

In this paper, the fundamental imaging physics of immersion lithography will be described. The impact of resolution and depth of focus will be explored, as well as the subtle though significant influence of hyper NAs on polarization related thin film effects and the definition of intensity. With a rigorous model in place, the use of immersion lithography for extending 193nm towards its ultimate limits will be explored.

Keywords: Immersion Lithography, Lithography Simulation, PROLITH

1. Introduction and Theory

Although the scientific principles underlying immersion lithography have been know for well over 100 years, only recently has this technology attracted widespread attention in the semiconductor industry. Despite this rather late start, the potential of immersion lithography for improved resolution and depth of focus is changing the industry's roadmap and seems destined to extend the life of optical lithography to new, smaller limits.

The story of immersion lithography begins with Snell's Law. Light traveling through material 1 with refractive index n_1 strikes a surface with angle θ_1 relative to the normal to that surface. The light transmitted into material 2 (with index n_2) will have an angle θ_2 relative to that same normal as given by Snell's law.

$$n_1 \sin\theta_1 = n_2 \sin\theta_2 \tag{1}$$

* chris.a.mack@kla-tencor.com, KLA-Tencor, 8834 N. Capital of Texas Highway, Suite 301, Austin, TX 78759 USA

Now picture this simple law applied to a film stack made of up any number of thin parallel layers (Figure 1a). As light travels through each layer Snell's law can be repeatedly applied:

$$n_1 \sin\theta_1 = n_2 \sin\theta_2 = n_3 \sin\theta_3 = n_4 \sin\theta_4 = \ldots = n_k \sin\theta_k \qquad (2)$$

Thanks to Snell's law, the quantity $n\sin\theta$ is *invariant* as a ray of light travels through this stack of parallel films. Interestingly, the presence or absence of any film in the film stack in no way affects the angle of the light in other films of the stack. If films 2 and 3 were removed from the stack in Figure 1a, for example, the angle of the light in film 4 would be exactly the same.

We find another, related invariant when looking at how an imaging lens works. A well made imaging lens (with low levels of aberrations) will have a *Lagrange invariant* (often just called the optical invariant) that relates the angles entering and exiting the lens to the magnification m of that lens.

$$m = \frac{n_o \sin\theta_o}{n_i \sin\theta_i} \qquad (3)$$

where n_o is the refractive index of the media on the object side of the lens, θ_o is the angle of a ray of light entering the lens relative to the optical axis, n_i is the refractive index of the media on the image side of the lens, and θ_i is the angle of a ray of light exiting the lens relative to the optical axis (Figure 1b). Note that, other than a scale factor given by the magnification of the imaging lens and a change in the sign of the angle to account for the focusing property of the lens, the Lagrange invariant makes a lens seem like a thin film obeying Snell's law. (It is often convenient to imagine the imaging lens as 1X, scaling all the object dimensions by the magnification, thus allowing m = 1 and making the Lagrange invariant look just like Snell's law).

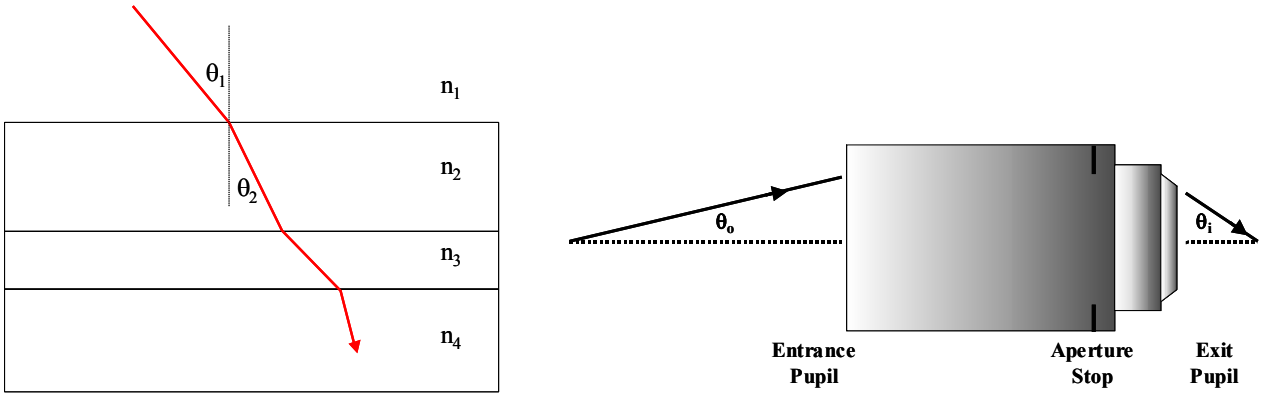

(a) (b)

Figure 1. Two examples of an "optical invariant", a) Snell's law of refraction through a film stack, and b) the Lagrange invariant of angles propagating through an imaging lens.

These two invariants can be combined when thinking about how a photolithographic imaging system works. Light diffracts from the mask (the object of the imaging lens) at a particular angle. This diffracted order propagates through the lens and emerges at an angle given by the Lagrange invariant. This light then

propagates through the media between the lens and the wafer and strikes the photoresist. Snell's law dictates the angle of that ray in the resist, or any other layers that might be coated on the wafer. Taking into account the magnification scale factor, the quantity $n\sin\theta$ for a diffracted order is constant from the time it leaves the mask to the time it combines inside the resist with other diffraction orders to form an image of the mask.

So how does this optical invariant affect our understanding of immersion lithography? If we replace the air between the lens and the wafer with water, the optical invariant says that the angles of light inside the resist will be the same, presumably creating the exact same image. Is there then no impact of immersion lithography? There is, from two sources: the maximum possible angle of light that can reach the resist, and the phase of that light.

Consider again the chain of angles through multiple materials as given by equation (2). Trigonometry will never allow the sine of an angle to be greater than one. Thus, the maximum value of the invariant will be limited by the material in the stack with the smallest refractive index. If one of the layers is air (with a refractive index of 1.0), this will become the material with the smallest refractive index and the maximum possible value of the invariant will be 1.0. If we look then at the angles possible inside of the photoresist, the maximum angle possible would be $\sin\theta_{\max,resist} = 1/n_{resist}$. Now suppose that the air is replaced with a fluid of a higher refractive index, but still smaller than the index of the photoresist. In this case, the maximum possible angle of light inside the resist will be greater: $\sin\theta_{\max,resist} = n_{fluid}/n_{resist}$. At a wavelength of 193nm, resists have refractive indices of about 1.7 and water has a refractive index of about 1.44. The fluid does not make the angles of light larger, but it *enables* those angles to be larger. If one were to design a lens to emit larger angles, immersion lithography will allow those angles to propagate into the resist. The numerical aperture of the lens (defined as the maximum value of the invariant $n\sin\theta$ that can pass through the lens) can be made to be much larger using immersion lithography, with the resulting improvements in resolution one would expect.

The second way that an immersion fluid changes the results of imaging comes from the how the fluid affects the phase of the light as it reaches the wafer. Light, being a wave, undergoes a phase change as it travels. If light of (vacuum) wavelength λ travels some distance Δz through some material of refractive index n, it will undergo a phase change $\Delta\phi$ given by

$$\Delta\varphi = 2\pi n\Delta z/\lambda \tag{4}$$

A phase change of 360º will result whenever the optical path length (the refractive index times the distance traveled) reaches one wavelength. This is important in imaging when light from many different angles combine to form one image. All of these rays of light will be in phase only at one point – the plane of best focus. When out of focus, rays traveling at larger angles will undergo a larger phase change than rays traveling at smaller angles. As a result, the phase difference between these rays will result in a blurred image.

How does immersion lithography affect this picture? For a given diffraction order (and thus a given angle of the light inside the resist), the angle of the light inside an immersion fluid will be less than if air were used. These smaller angles will result in smaller optical path differences between the various diffracted orders when out of focus, and thus a smaller degradation of the image for a given amount of defocus. In other words, for a given feature being printed and a given numerical aperture, immersion lithography will provide a greater depth of focus (DOF). A more thorough description of the impact of immersion on DOF will be given in the following section.

2. Immersion and the Depth of Focus

Lord Rayleigh, more than 100 years ago, gave us a simple approach to estimating depth of focus in an imaging system. Here we'll expressing his method and results in modern lithographic terms, as well as extend them to numerical apertures appropriate to immersion lithography.

A common way of thinking about the effect of defocus on an image is to consider the defocusing of a wafer as equivalent to causing an aberration – an error in curvature of the actual wavefront relative to the desired wavefront (i.e., the one that focuses on the wafer). The distance from the desired to the "defocused" wavefront goes from zero at the center of the exit pupil and increases as we approach the edge of the pupil. This distance between wavefronts is called the *optical path difference* (OPD). The OPD is a function of the defocus distance δ and the position within the pupil and can be obtained from the geometry of a converging spherical wave. Describing the position within the exit pupil by an angle θ, the optical path difference is given (after a bit of geometry and algebra) by

$$OPD = \delta(1 - \cos\theta) \tag{5}$$

Depth of focus (DOF) is defined generically as the range of focus that can be tolerated. While an exact criterion for "tolerated" is application dependent, a simple example can be used to guide a basic description of DOF. Consider the imaging of an array of small lines and spaces. The diffraction pattern for such a mask is a set of discrete diffraction orders, points of light entering the lens spaced regularly depending only on the wavelength of the light λ and the pitch p of the mask pattern. The angles at which these diffraction orders will emerge from the lens are given by Bragg's condition:

$$\sin\theta = \frac{m\lambda}{p} \tag{6}$$

where m is an integer. Using this integer to name the diffraction orders, a high resolution pattern of lines and spaces will result in only the zero and the plus and minus first diffraction orders passing through the lens to forming the image.

Combining equations (5) and (6) we can see how much *OPD* will exist between the zero and first orders of our diffraction pattern. Unfortunately, some trigonometric manipulations will be required to convert the cosine of equation (5) into the more convenient sine of equation (6). One such manipulation uses a Taylor series:

$$OPD = \delta(1 - \cos\theta) = \frac{1}{2}\delta\left(\sin^2\theta + \frac{\sin^4\theta}{4} + \frac{\sin^6\theta}{8} + \ldots\right) \tag{7}$$

At the time of Lord Rayleigh, lens numerical apertures were relatively small. Thus, the largest angles going through the lens were also quite small and the higher order terms in the Taylor series could be safely ignored, giving

$$OPD \approx \frac{1}{2}\delta\sin^2\theta \tag{8}$$

How much OPD can our line/space pattern tolerate? Consider the extreme case. If the *OPD* were set to a quarter of the wavelength, the zero and first diffracted orders would be exactly 90º out of phase with

each other. At this much *OPD*, the zero order would not interfere with the first orders at all and no pattern would be formed. The true amount of tolerable *OPD* must be less than this amount.

$$OPD_{\max} = k_2 \frac{\lambda}{4}, \quad where\ k_2 < 1 \tag{9}$$

Substituting this maximum permissible *OPD* into equation (8), we can find the DOF.

$$DOF = 2\delta_{\max} = k_2 \frac{\lambda}{\sin^2 \theta} \tag{10}$$

At this point Lord Rayleigh made a crucial application of this formula that is often forgotten. While equation (10) would apply to any small pattern of lines and spaces (that is, any pitch applied to equation (6) so that only the zero and first orders go through the lens), Lord Rayleigh essentially looked at the extreme case of the smallest pitch that could be imaged – the resolution limit. The smallest pitch that can be printed would put the first diffracted order at the largest angle that could pass through the lens, defined by the numerical aperture, *NA*. For this one pattern, the general expression (10) becomes the more familiar and specific Rayleigh DOF criterion:

$$DOF = k_2 \frac{\lambda}{NA^2} \tag{11}$$

From the above derivation we can state the restrictions on this conventional expression of the Rayleigh DOF: relatively low numerical apertures imaging a binary mask pattern of lines and spaces at the resolution limit. To lift some of these restrictions we simply use the exact OPD expression and leave the angle to be defined by equation (6) [1].

$$DOF = \frac{k_2}{2} \frac{\lambda}{(1-\cos\theta)} = \left(\frac{k_2}{4}\right) \frac{\lambda}{\sin^2\left(\frac{\theta}{2}\right)} \tag{12}$$

This high NA version of the Ralyeigh DOF criterion still assumes we are imaging a small binary pattern of lines and spaces, but is appropriate at any numerical aperture. It can also be modified to account for immersion lithography quite easily. When the space between the lens and the wafer is filled with a fluid of refractive index n_{fluid}, the optical path difference becomes the physical path different multiplied by this refractive index. Thus equation (5) becomes

$$OPD = n_{fluid}\, \delta(1-\cos\theta) \tag{13}$$

and the high NA version of the Rayleigh criterion becomes

$$DOF = \frac{k_2}{2} \frac{\lambda}{n_{fluid}\,(1-\cos\theta)} \tag{14}$$

Likewise, the angle θ can be related to the pitch by the modification of equation (6) to account for immersion.

$$n_{fluid} \sin\theta = \frac{m\lambda}{p} \tag{15}$$

Combining equations (14) and (15) one can see how immersion will improve the depth of focus of a given feature:

$$\frac{DOF(immersion)}{DOF(dry)} = \frac{1-\sqrt{1-(\lambda/p)^2}}{n_{fluid}-\sqrt{(n_{fluid})^2-(\lambda/p)^2}} \tag{16}$$

As Figure 2 shows, the improvement in DOF is at least the refractive index of the fluid, and grows larger from there for the smallest pitches. It's no wonder immersion lithography is attracting so much attention.

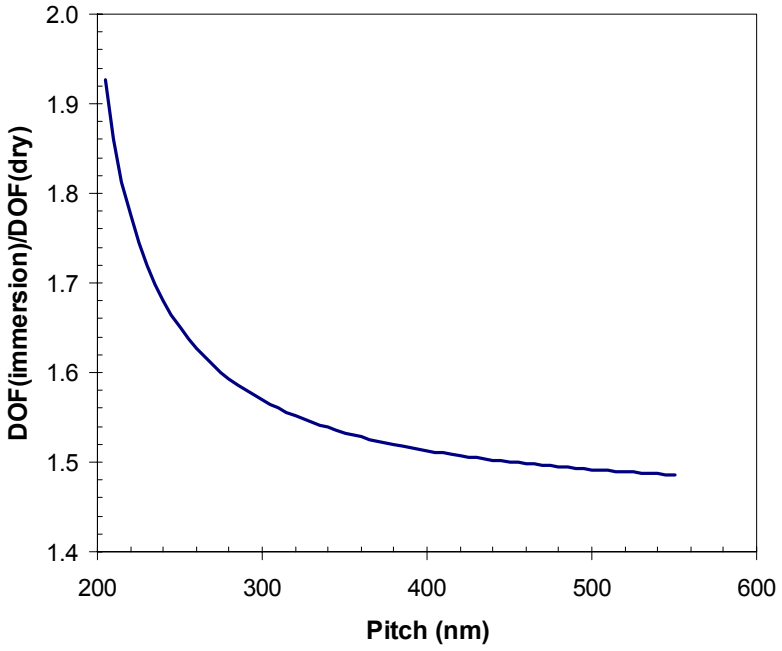

Figure 2. For a given pattern of small lines and spaces, using immersion improves the depth of focus by at least the refractive index of the fluid (in this example, λ = 193nm, n_{fluid} = 1.46).

3. Polarization, Reflectivity, and the Definition of Intensity

The high angle propagation and interference of light that results from very high numerical apertures presents several challenges, both in describing and calculating the nature of this light, and in controlling the light to achieve desired lithographic results. When two planes interfere, the amount of interference is determined by the amount the two electric fields overlap (i.e., by the dot product of the electric field vectors). When the angle between the two plane waves is small, the electric field overlap is nearly 100% and the vector sum of the electric fields is nearly equal to the scalar sum (Figure 3). However, as the angle increases the amount of overlap becomes dependent on the direction of the electric field vector. Although unpolarized light contains

all possible electric field vector directions that are perpendicular to the direction of travel, mathematically we can decompose an unpolarized wave into the incoherent sum of any two orthogonal polarizations. Since we will be interested in how a plane wave propagates into a resist coated wafer, the two most convenient directions are those parallel and perpendicular to the plane of intersection of the waves with the film, as described in more detail below. Thus, a description of the polarization direction of the light becomes an integral part of how images form inside of a photoresist film.

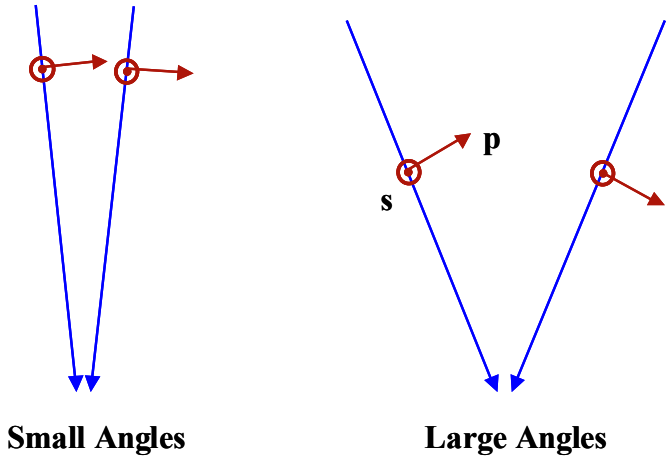

Figure 3. The overlap of s-polarized (TE) light is always perfect, regardless of the angle between the waves. For p-polarized (TM) light, the amount of overlap (and thus interference) decreases as the angle increases.

While seemingly simple in concept, the definition of light intensity is more complicated than expected. In particular, a comparison of intensity values when the light is in different materials and traveling at different angles requires careful consideration. One case where these difficulties become apparent is the simple refraction of a plane wave traveling from one medium to another. Thus, our discussion will begin with a look at electric field and intensity reflection and transmission coefficients. The following derivations are based on the standard treatment given by Born and Wolf [2]. (Note, however, that many modern authors do not follow Born and Wolf's use of the words *intensity* and *irradiance*, though few would dispute the correctness of the physics that they present.)

Consider light intersecting the plane interface between two materials, numbered 1 and 2 as shown in Figure 4. For the moment we will consider normal incidence of the light on this interface, with an incident electric field E_i, a reflected electric field E_r, and a transmitted electric field E_t. The electric field reflection and transmission coefficients at normal incidence are given by

$$\rho_{12} = \frac{E_r}{E_i} = \frac{\boldsymbol{n}_1 - \boldsymbol{n}_2}{\boldsymbol{n}_1 + \boldsymbol{n}_2}$$

$$\tau_{12} = \frac{E_t}{E_i} = \frac{2\boldsymbol{n}_1}{\boldsymbol{n}_1 + \boldsymbol{n}_2} \tag{17}$$

where $\boldsymbol{n}_j = n_j + i\kappa_j$ = the complex index of refraction of material j.

The transmission and reflection coefficients are also functions of the angle of incidence and the polarization of the incident light. If θ_i is the incident (and reflected) angle and θ_t is the transmitted angle, then the electric field reflection and transmission coefficients are given by the Fresnel formulae.

$$\rho_{12\perp} = \frac{\boldsymbol{n}_1 \cos(\theta_i) - \boldsymbol{n}_2 \cos(\theta_t)}{\boldsymbol{n}_1 \cos(\theta_i) + \boldsymbol{n}_2 \cos(\theta_t)}$$

$$\tau_{12\perp} = \frac{2\boldsymbol{n}_1 \cos(\theta_i)}{\boldsymbol{n}_1 \cos(\theta_i) + \boldsymbol{n}_2 \cos(\theta_t)}$$

$$\rho_{12\|} = \frac{\boldsymbol{n}_1 \cos(\theta_t) - \boldsymbol{n}_2 \cos(\theta_i)}{\boldsymbol{n}_1 \cos(\theta_t) + \boldsymbol{n}_2 \cos(\theta_i)}$$

$$\tau_{12\|} = \frac{2\boldsymbol{n}_1 \cos(\theta_i)}{\boldsymbol{n}_1 \cos(\theta_t) + \boldsymbol{n}_2 \cos(\theta_i)} \qquad (18)$$

Here, $\|$ represents an electric field vector which lies parallel to the plane defined by the direction of the incident light and a normal to the material interface (i.e., in the plane of the paper in Figure 4). Other names for $\|$ polarization include *p* polarization and TM (transverse magnetic) polarization. The polarization denoted by $\perp$ represents an electric field vector which lies in a plane perpendicular to that defined by the direction of the incident light and a normal to the surface (i.e., perpendicular to the plane of the paper in Figure 4). Other names for $\perp$ polarization include *s* polarization and TE (transverse electric) polarization. Note that for light normally incident on the resist surface, both *s* and *p* polarization result in electric fields which lie along the resist surface and the four Fresnel formulae revert to the two standard definitions of normal incidence reflection and transmission coefficients given in equation (17).

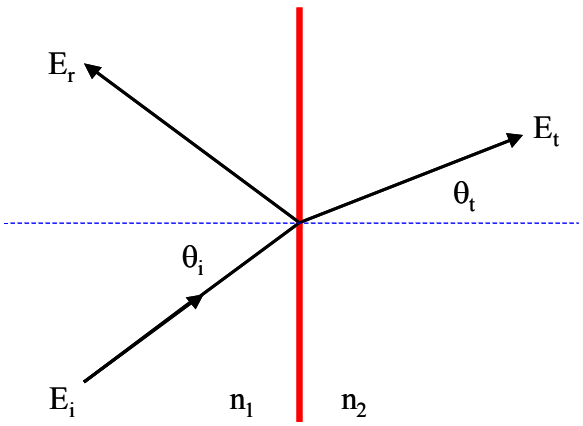

Figure 4. Geometry used for the definition of Snell's law and reflection and transmission coefficients.

It is interesting to look at the impact of the direction that the light is traveling on the definitions of equation (17). Completely reversing the direction of the light in Figure 4, if light approaches the interface through material 2 at an angle θ_t, the resulting reflection and transmission coefficients become

$$\rho_{21} = -\rho_{12}$$

$$\tau_{21} = \frac{\boldsymbol{n}_2 \cos(\theta_t)}{\boldsymbol{n}_1 \cos(\theta_i)} \tau_{12} \tag{19}$$

where these relationships hold for either polarization.

The difference between intensity and irradiance is a subtle one, and notwithstanding the different definitions of these terms in use today, when determining the intensity or irradiance transmitted into a material at an oblique angle it is very important to differentiate between the two. I will define the intensity of light as the magnitude of the (time averaged) Poynting vector, the energy per second crossing a unit area perpendicular to the direction of propagation of the light. It is given by

$$I = n|E|^2 \tag{20}$$

where *n* is the real part of the refractive index of the media. Note that the definition given in equation (20) may differ by a constant multiplicative factor depending on the units used. The irradiance is the projection of the intensity onto a surface which may not be normal to the direction that the light is traveling.

The intensity reflectivity and transmission, for either polarization, are derived by considering a unit area on the interface between the two materials. Consider the irradiance, J, of the incident light along the surface of the interface between the materials.

$$J_i = I_i \cos(\theta_i) \tag{21}$$

Likewise, the irradiances of the reflected and transmitted light along this surface are

$$\begin{aligned} J_r &= I_r \cos(\theta_i) \\ J_t &= I_t \cos(\theta_t) \end{aligned} \tag{22}$$

Now the irradiance reflectivity and transmission coefficients can be defined

$$R_{12} = R_{21} = R = \frac{J_r}{J_i} = |\rho_{12}|^2$$

$$T_{12} = T_{21} = T = \frac{J_t}{J_i} = \frac{n_2 \cos(\theta_t)}{n_1 \cos(\theta_i)} |\tau_{12}|^2 \tag{23}$$

From these two equations it is easy to show that R + T = 1 for each polarization, which is a consequence of conservation of energy. Figure 5 shows how the irradiance reflectivity varies with incident angle for both *s* and *p* polarized illumination. An alternate form for equations (23), making use of the reverse direction definitions of reflection and transmission coefficients in equation (19), are

$$R = |\rho_{12}\ \rho_{21}|$$

$$T = \left|\tau_{12}\,\tau_{21}\right| \tag{24}$$

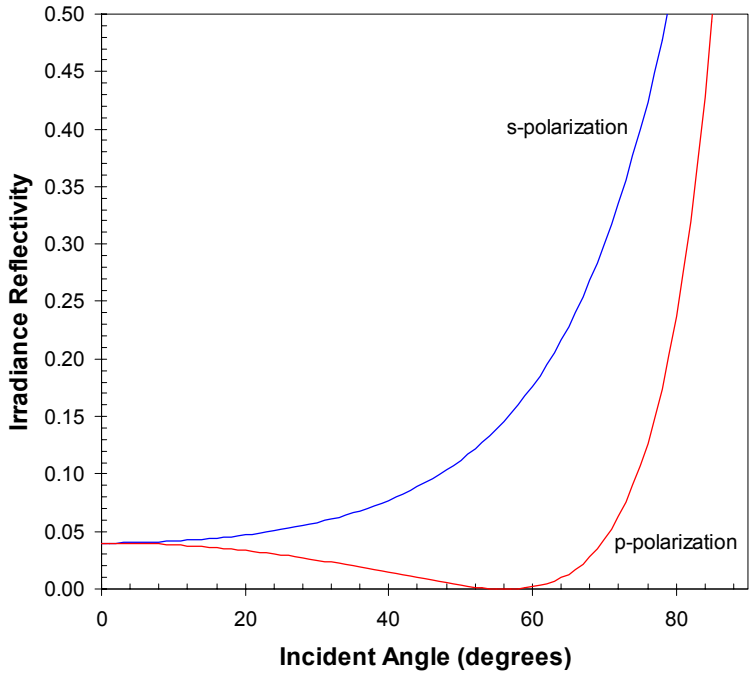

Figure 5. Reflectivity (square of the reflection coefficient) as a function of the angle of incidence showing the difference between *s* and *p* polarization (n_1 = 1.0, n_2 = 1.5).

Consider a unit intensity plane wave incident on the plane boundary between material 1 and 2 at an incident angle θ_i and with intensity I_i. From equation (20) the magnitude of the incident electric field must be

$$\left|E_i\right| = \sqrt{\frac{I_i}{n_1}} \tag{25}$$

The transmitted electric field is then

$$\left|E_t\right| = \left|\tau_{12} E_i\right| = \left|\tau_{12}\right| \sqrt{\frac{I_i}{n_1}} \tag{26}$$

The transmitted intensity (i.e., the intensity in material 2) is found by applying the definition of intensity to equation (26).

$$I_t = n_2 \left|E_t\right|^2 = \frac{n_2}{n_1} \left|\tau_{12}\right|^2 I_i \tag{27}$$

By comparing equation (27) with equation (23), the non-intuitive result below is obtained.

$$I_t = T\frac{\cos(\theta_1)}{\cos(\theta_2)}I_i \tag{28}$$

As can be seen in equation (28), the transmittance T is not the ratio of the intensities I_t and I_i (see Figure 6). The difference comes from the change in the direction of the energy flow caused by refraction. Thus, one might ask the question, which is more important to know inside film 2, the intensity of the plane wave, or its irradiance along a surface parallel to the material interface? The answer to this question depends on the task at hand. For lithography simulation (and, in fact, most physics problems) it is the absorbed energy that determines the effects of exposure to light. The absorbed energy is calculated by the Lambert law of absorption, using a definition of intensity as given above, that is, the energy flow through an area perpendicular to the direction of travel. Thus, for lithography simulation, the intensity as defined in equation (20) is the quantity that matters.

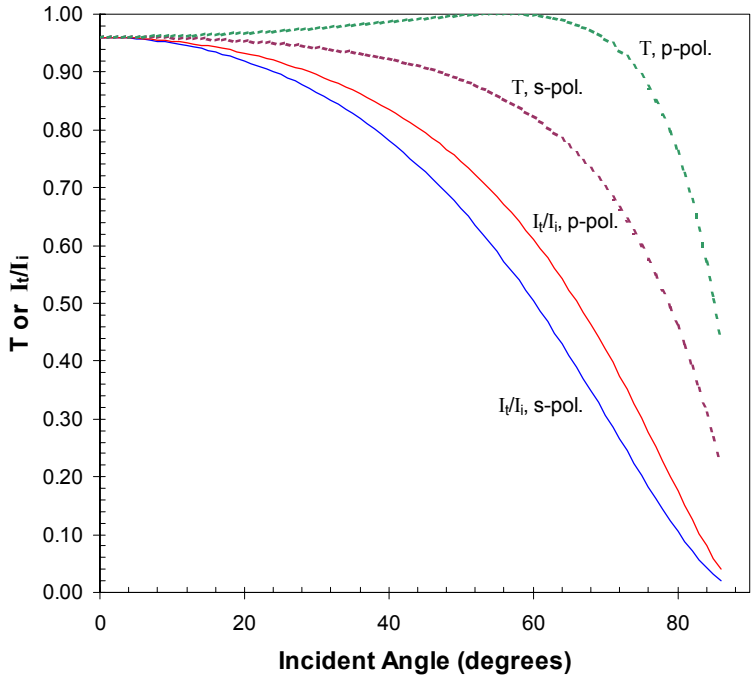

Figure 6. Intensity transmitted into layer 2 relative to the incident intensity (solid lines) and the transmittance T (dashed lines) as a function of the angle of incidence for both *s* and *p* polarization (n_1 = 1.0, n_2 = 1.5).

Note, however, that although the irradiance transmittance T is not an accurate predictor of the fraction of the intensity of light making it in to the film, the ratio T_s/T_p is the same as the ratio of *s* and *p* intensities inside the film for an unpolarized incident wave.

4. Simulations

Vector simulations that accurately track the polarization vectors of the electric fields that propagate from the lens to and through the film stack on the wafer allow the hyper-NAs of future immersion lithography systems to be accurately modeled. For the simulations presented below, PROLITH v8.1 from KLA-Tencor was used. Figure 7 shows how the use of immersion can greatly improve the process window and depth of focus when printing the same features at the same numerical aperture. Figures 8 and 9 shows how, for the case of immersion with dipole illumination, picking an optimum polarization direction for the illumination can improve the process window.

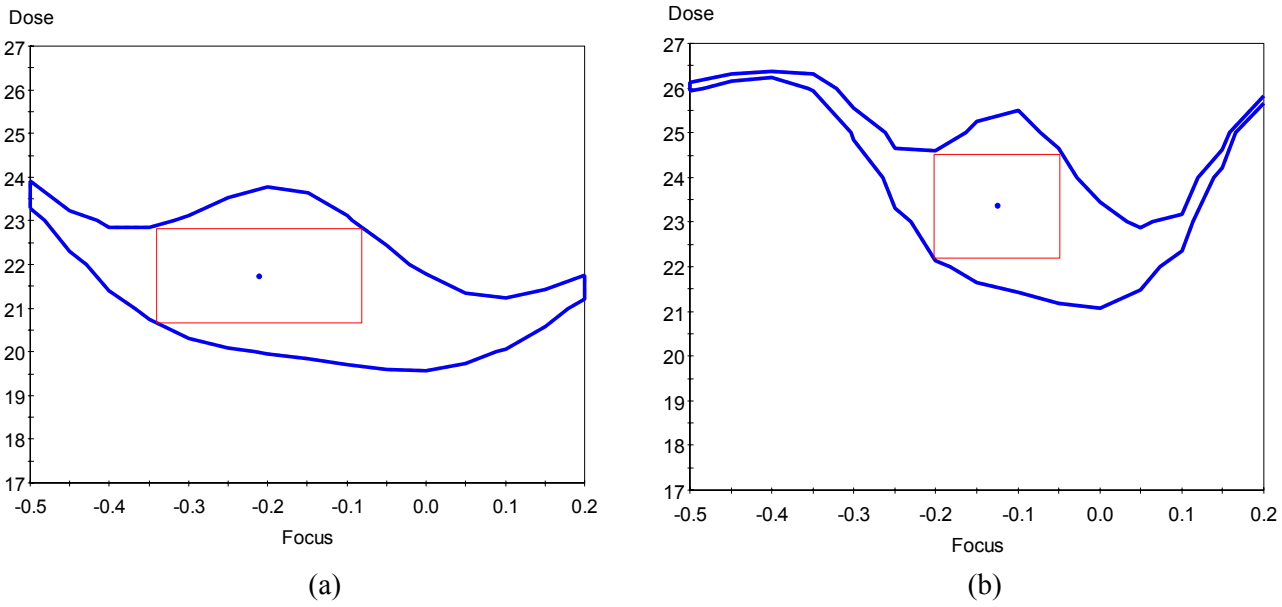

Figure 7. For a given NA, immersion lithography can greatly improve the depth of focus (193nm, NA = 0.9, σ = 0.7 (unpolarized), 90nm lines, 250nm pitch): a) immersion, and b) dry.

Although Figures 8 and 9 show clearly the benefits of avoiding the "wrong" polarization, the polarization direction that results in *p*-polarization at the wafer, these examples make use of an extreme case: dipole illumination when only one orientation of lines and spaces occurs on the mask. To avoid a double exposure process, some form of quadrupole or annular illumination must be used. One option is the so-called double dipole or cross quad as show in Figure 10. By making the illumination azimuthally polarized, each pole can have the optimum polarization for the orientation of lines and spaces that it is intended for. As can be seen in Figure 10, the use of azimuthal polarization significantly improves the exposure latitude and somewhat improves the depth of focus for these 110nm pitch patterns.

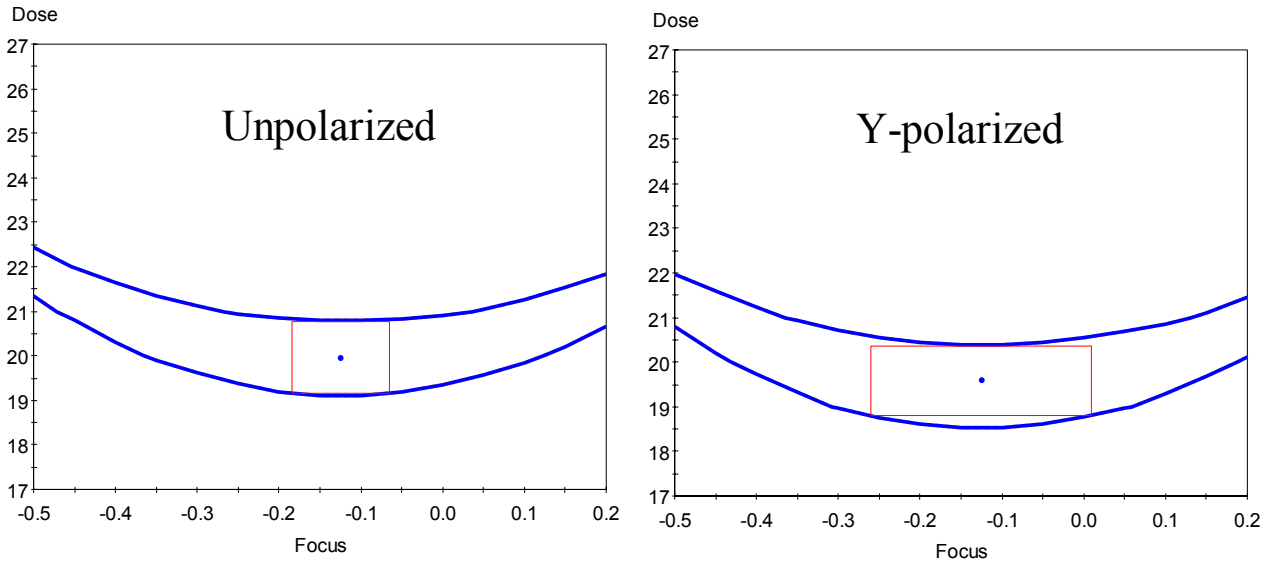

Figure 8. Polarization affects reduce the size of the process window (immersion, 193nm, NA = 0.9, Dipole σ = 0.6/0.2, 90nm lines, 180nm pitch). When the optimum polarization direction for the illumination is chosen, the best process window is obtained.

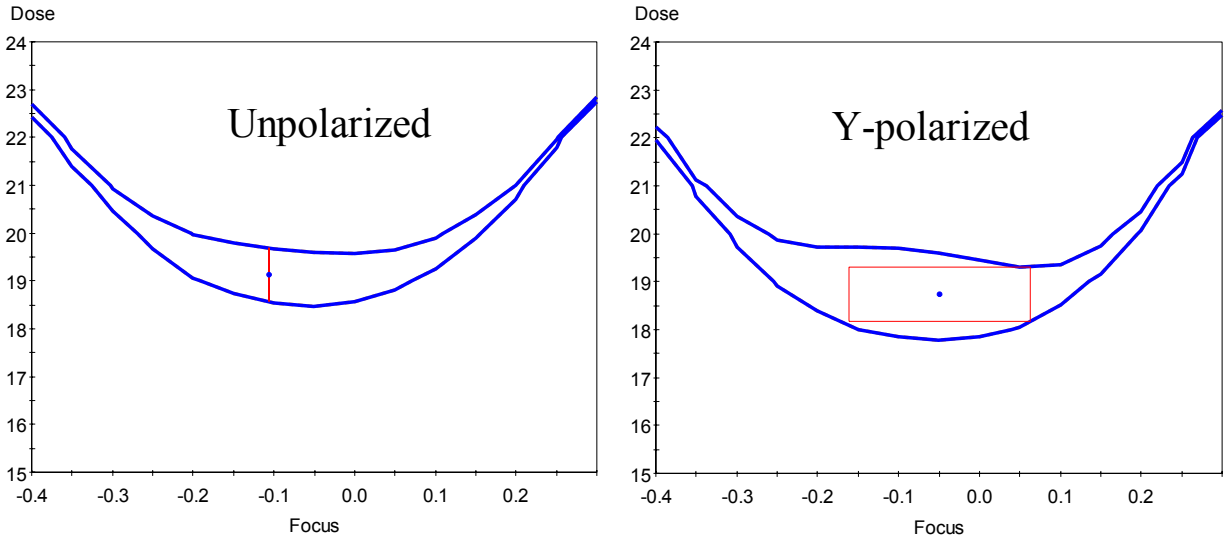

Figure 9. Polarization affects reduce the size of the process window (immersion, 193nm, NA = 1.2, Dipole σ = 0.6/0.2, 50nm lines, 130nm pitch). When the optimum polarization direction for the illumination is chosen, the best process window is obtained.

5. Conclusions

Immersion lithography shows great potential for increasing the depth of focus of a process at a given resolution. An increase in DOF of at least the refractive index of the fluid can be obtained, though up to a

doubling of the DOF is possible at the smallest pitches. Further, the use of immersion enables the design and construction of "hyper NA" lens, lens with numerical apertures greater than 1. Immersion, however, will not stop the progression of complexity and cost that the trend to higher NAs has always followed. These hyper-NA lens will required continued dramatic improvements in lens design and manufacturing technology. These improvements seem likely, though, and numerical apertures up to 1.2 seem likely, and NAs of 1.3 seem possible with water immersion at 193nm.

The hyper NAs enabled by immersion lithography pose another challenge to the lithographic system developer. The full resolution benefits of these higher NAs can only be realized when the optimum polarization of the illumination is used. Thus, illumination polarization control (IPC) will become a necessary component of a hyper NA immersion tool. Azimuthal polarization may be a good compromise for cross quad and annular illumination systems, though polarization may need to be optimized more fully for the wide variety of source shapes that may be used for the extreme lithographic imaging conditions of the future.

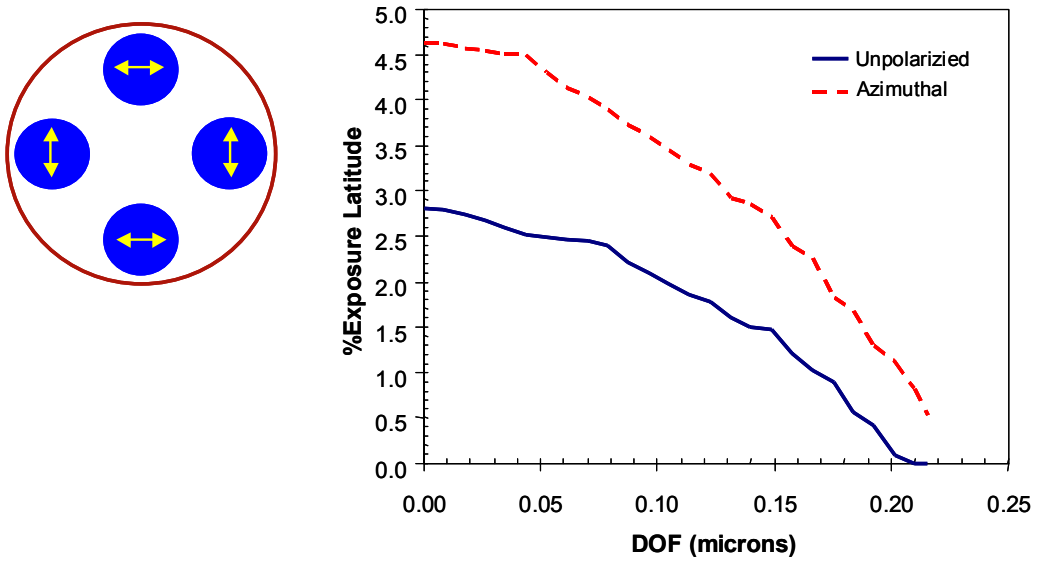

Figure 10. Azimuthal polarization is one option for minimizing the detrimental affects of the "wrong" polarization when dipole illumination is not an option (193nm, NA = 1.2, Cross-quad σ = 0.73/0.2, 50nm lines, 110nm pitch).

References

1. B. J. Lin, "The k_3 Coefficient in Nonparaxial λ/NA Scaling Equations for Resolution, Depth of Focus, and Immersion Lithography," *Journal of Microlithography, Microfabrication, and Microsystems*, Vol. 1, No. 1 (April 2002) pp. 7-12.
2. M. Born and E. Wolf, Principles of Optics, 6th edition, Pergamon Press, (Oxford, 1980) pp. 41.